ISSN: 2688-8645

Study on the Lower Bound of Reservoir Properties in the L Member of the Lower White Poplar River Formation, Tertiary System, Yaxia Oilfield

Liang Chen [1, 2], Qinlian Wei [1, 2], Yanxin Bao [3], Chengqian Tan [1, 2]

[1] School of Earth Sciences and Engineering, Xi'an Shiyou University, Xi'an, Shaanxi 710065, China

[2] Shaanxi Key Laboratory of Petroleum Accumulation Geology, Xi'an Shiyou University, Xi'an, Shaanxi 710065, China

[3] Seventh Oil Production Plant, Changqing Oilfield Company, PetroChina, Xi'an, Shaanxi 710200, China

Abstract

Addressing the ambiguity surrounding the lower limits of effective reservoir properties in the L Member of the Biaoyanghe Formation, Tertiary System, in the Yaxia area, this study employs a multidisciplinary approach integrating property data, logging interpretation results, sedimentary facies analysis, and cast thin sections. It investigates the lower limits of effective reservoir properties and analyzes the primary factors governing their development. The study indicates that the lower limits for the L Member in the study area are: , porosity 8.2%, and permeability 1.5$^{\times 10^{-3} \mu m^2}$.

Keywords

Effective Reservoir; Minimum Physical Properties; Controlling Factors; Baiyanghe Formation; Yaxia Area.

1. Introduction

The Yaxia Oilfield is a typical tectonic-lithologic hydrocarbon reservoir, where tectonics, lithofacies, and faults are the three primary factors controlling hydrocarbon accumulation in the L reservoir. Tectonically favorable zones constitute the primary hydrocarbon accumulation areas; subaqueous distributary channels, estuarine bars, and sheet-like sand deposits form the effective hydrocarbon reservoirs; Faults serve as primary migration pathways for hydrocarbons. Simultaneously, the complex interplay of numerous faults and sandstone distribution patterns results in heterogeneous hydrocarbon distribution within the reservoir. Blocks where structurally favorable zones, fault development, and the distribution of subaqueous deltaic channels and deltaic fan sandstones align constitute favorable hydrocarbon accumulation areas.

The reservoir distribution in lithostructural hydrocarbon reservoirs is dual-controlled by lithological variations and tectonic actions (e.g., sandstone termination, fault blocking), exhibiting strong heterogeneity. Through lower limit analysis of physical properties, the scope of effective reservoir space can be delineated, preventing misclassification of ineffective low-permeability zones as exploitable targets.

In recent years, scholars worldwide have progressively developed multiple methods for determining effective reservoir property lower limits based on dynamic production data and core experimental analysis. Wu et al. used nuclear magnetic resonance centrifuge testing to define the property lower limits for tight lacustrine carbonate reservoirs in the western Qaidam Basin [1]; Zhang Yuxiang et al. applied radial flow productivity simulation to determine the lower limits of physical properties for ultra-deep carbonate reservoirs in the Deng IV Member of the Sichuan Basin [2];; Cheng Qi et al. used the hydrocarbon-filling pressure equilibrium method to define the lower limits of reservoir properties for tight reservoirs in the Fengcheng Formation of the Lower Permian in the Fengcheng area of the Junggar Basin, systematically revealing the coupling relationship between reservoir property lower limits and burial depth in the study area [3]; Li Wenhao et al. comprehensively employed the functional curve method and oil testing to define the lower limits of effective reservoir properties for gravels in the northern Bohai Sea, further elucidating the composite control mechanism of sedimentary environment, diagenetic evolution, and formation pressure on reservoir development from a petrogenetic perspective [4].; Cao Yingchang et al. significantly enhanced the reliability of reservoir evaluation through synergistic validation using empirical statistical methods, well testing, distribution function curve analysis, and pore permeability correlation [5].

2. Geological Overview

The Ya'erxia Oilfield is situated on the southern thrust syncline structure of the Jiuxi Basin, bordering the Qingxi Depression to the west, connecting to the Laojunmiao Anticline to the east, adjacent to the Yanbei Uplift to the north, and proximate to the Qilian Mountains to the south. Geological records and prior analyses of tectonic evolution indicate that the structural basement comprises Early Paleozoic metamorphic rocks and Late Paleozoic sandstones and mudstones. During the early Yanshanian orogeny, faults developed in the southwest basin, depositing Jurassic fluvial strata. Lithologies primarily include conglomerates, sandstones, mudstones, and coal-bearing rocks from fluvial-lacustrine environments. In the Late Jurassic, the graben rift reversed and uplifted, eroding the Upper Jurassic strata and leaving only Middle-Lower Jurassic deposits.

During the mid-Yanshanian orogeny, the basin underwent renewed extensional stress on the Jurassic rift base. This formed three east-west trending rifts—the Qingxi, Shibei, and Dahongquan depressions—controlled by northeast-trending normal faults. In the late Yanshanian, basin uplift prevented Upper Cretaceous deposition.

During the Himalayan Orogeny, the three basins first subsided, forming a larger basin where Tertiary strata were deposited. The Lower Tertiary strata unconformably overlie the Lower Cretaceous. Concurrently, tectonic stress shifted from tensional to compressional forces. This generated two sets of reverse faults trending northwest and northeast, along with local structures such as Qingxi, Yaxia, and Laojunmiao.

3. Reservoir Characteristics

Based on core observations from drilling and petrographic analysis, the L reservoir in the Yaxia Oilfield primarily consists of a terrestrial clastic sequence—a sandstone-mudstone sequence. The rock colors predominantly range from reddish-brown, dark purplish-red, brown, and light gray, with minor intercalations of light red, grayish-green, and grayish-white. The reservoir lithology is dominated by calcareous and siliceous fine sandstones and muddy, carbonate-bearing siltstones, exhibiting good oil retention with widespread oil saturation and oil spots. Secondary lithologies include muddy siltstones and minor medium-to-fine sandstones, which show poor oil retention with common oil traces and bands.

Based on data from 74 thin sections from wells 9851, 9811, and Ya5, the quartz content in the sandstone clastic components of the L reservoir ranges from 82% to 35%, with an average of 50.86%. Feldspar content ranged from 23% to 4%, averaging 11.06% (predominantly orthoclase); clastic content ranged from 60% to 1%, averaging 20.46%, exceeding feldspar content. The petrological types of sandstone are primarily feldspathic quartz sandstone and clastic quartz sandstone.

Table 1. Reservoir Pore Type Statistics

Pore Type	Lithological Designation	Clastic Component	Contact Characteristics
Intergranular Pores	Brownish-red fine-grained subplagioclase clastic sandstone	Quartzite, acidic volcanic rock, with iron-rich clay as matrix and calcite cement	Point contacts predominate between clasts, followed by free distribution; more common in the eastern part
Microporosity within matrix	Brownish-red, clay-rich, fine-grained clastic sandstone	Acidic volcanic rocks, quartzite, with minor granite	Intergranular pores poorly developed, with free-standing distribution and occasional microfractures
Microporosity within clasts	Grey-green carbonate-bearing silty sandstone	Primarily acidic volcanic rocks and quartzite, with iron-rich clay, mica, and chlorite as matrix components	Primarily distributed as free particles, followed by point contacts, more common in the western part
Interstitial microporosity	Gray to dark gray carbonate-rich muddy siltstone	Primarily acidic volcanic rocks, with minor quartzite, mica, and chlorite clay	Same as above

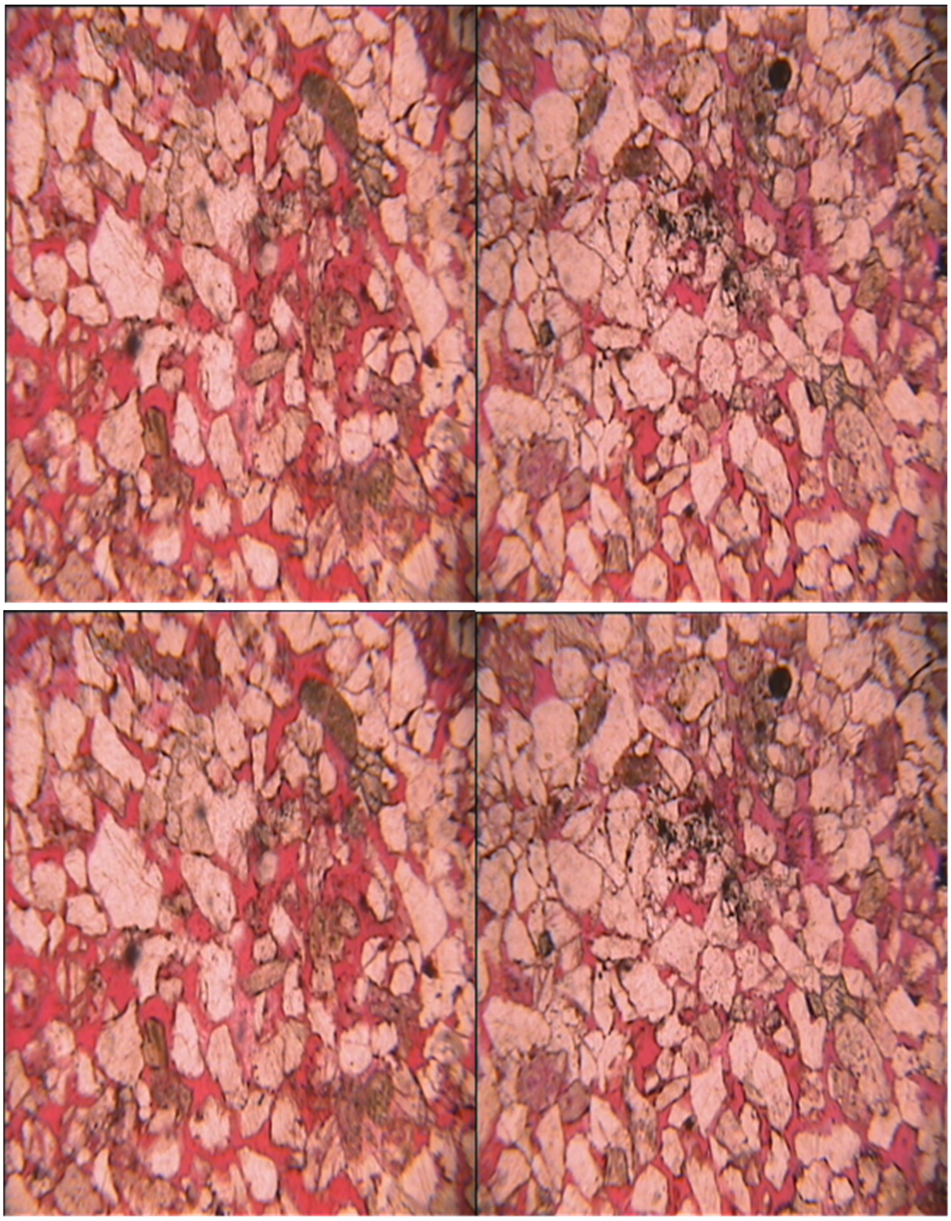

Figure 1. The reservoir exhibits poor porosity structure and strong heterogeneity

Impurities range from 18% to 1%, averaging 8%. Among cementing materials, carbonates (calcite, dolomite) dominate at 50% to 2%, averaging 11.16%, followed by kaolinite and gypsum at 12% to 1%, averaging 1.82%. Considering the overall rock composition, quartz constitutes 50.86%. Due to quartz's high hardness and good roundness, reservoir properties are favorable. However, clastic and cementing materials account for 20.46% and 11.16%, respectively. Since calcite, dolomite, and some impurities are soluble substances, they significantly impact reservoir properties. Cementation is predominantly pore-type, followed by matrix-pore-type, with minor pore-film-type cementation. Grain size ranges from 0.03 to 0.4 mm, exhibiting good to moderate sorting. Grain roundness is primarily subangular to subrounded, with a small proportion showing poor roundness.

Heavy minerals are dominated by hematite (65.5%), followed by pyrite (13.7%), garnet (7.5%), and magnetite with other minerals (12.16%).

In summary, the sandstone reservoirs of the Yaxia Oilfield exhibit characteristics of simple lithofacies, high clastic content, and relatively high rock maturity.

Based on scanning electron microscopy and cast thin section analyses from wells such as 9811 and 9851, the sandstone in this area primarily exhibits intergranular porosity supplemented by intergranular microporosity. Its types and characteristics are as follows: Analysis of core thin sections and other data indicates that the primary storage space in the Ya'erxia L reservoir consists of primary intergranular pores, followed by interbasal micropores and clastic micropores, with a small amount of intergranular dissolution pores also present (Table 1). The reservoir exhibits poor porosity structure and strong heterogeneity (Figure 1).

4. Determination of Lower Bound for Effective Reservoir Properties

4.1. Cumulative Frequency Method

The cumulative frequency method is based on the porosity and permeability of tight sandstones. It plots a histogram of porosity-permeability distribution frequencies, calculates reservoir energy storage and production capacity, and generates curves for cumulative sample loss frequency and cumulative energy storage loss frequency (Figure 2). The boundary for effective reservoirs is defined as a cumulative energy storage loss frequency of 5% in low-permeability reservoirs [6]. Analysis results indicate that at a cumulative energy loss frequency of 5%, the L-stage reservoir in the Yaxia area exhibits a porosity of 7.5% and a permeability of $1.^{2\times10^{-3}}\mu m^2$;

The calculation formula is as follows:

$$Q_{\varphi i}=\frac{\varphi_i H_i}{\sum_{i=1}^{n}\varphi_i H_i} \tag{1}$$

$$Q_{ki}=\frac{K_i H_i}{\sum_{i=1}^{n}K_i H_i} \tag{2}$$

$$Q\varphi=\sum_{i=1}^{n}Q\varphi i \tag{3}$$

$$Qk=\sum_{i=1}^{n}Qki \tag{4}$$

In Equations (1) to (4): $Q_{\varphi i}$ is the oil storage capacity calculated based on porosity, %; Q_{φ} is the oil storage capacity calculated based on permeability, %; H_i is the length of each sample, i.e., reservoir thickness, m; Q_{φ} is the cumulative oil production capacity derived from porosity, %; Q_k is the cumulative oil production capacity derived from permeability, %; n is the number of samples.

4.2. Bound Water Saturation Method

Field practice demonstrates that when fluids within reservoirs cannot permeate effectively, the bound water saturation typically exceeds 80%. At this point, the pore space of reservoir fluids primarily consists of microporosity. Therefore, using 80% bound water saturation as the cutoff value, the corresponding porosity and permeability are adopted as the lower limits for effective reservoir properties [7]. Figure 3 illustrates the relationship between bound water saturation and porosity. This diagram demonstrates a clear negative correlation between bound water saturation and porosity—bound water saturation increases as porosity decreases. This clearly indicates that as pores transition from effective to ineffective, fluid flow within the reservoir becomes significantly impeded. Based on the above analysis, the pore volume lower limit is set at 7.0%, corresponding to a bound water saturation of 80%. According to the pore-permeability relationship derived from core analysis, the corresponding lower limit of permeability is calculated to be 1.$^{1\times10^{-3}\mu m^2/m}$.

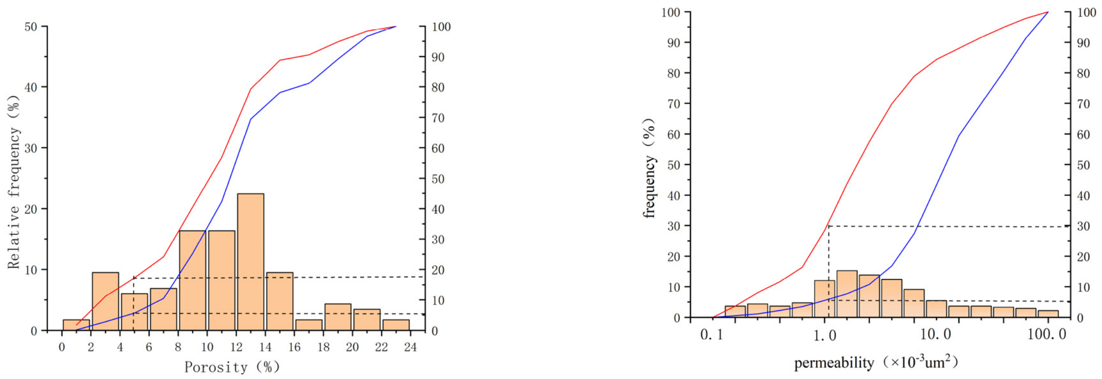

a. Pore Volume Frequency Distribution Histogram

b. Frequency distribution histogram of permeability

Figure 2. Pore Volume and Permeability Frequency Distribution Histogram

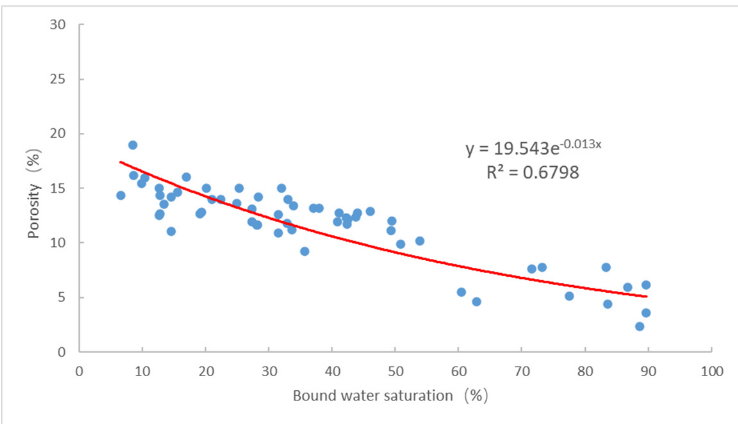

Figure 3. Boundary Water Saturation-Pore Volume Intersection Diagram

4.3. Displacement Pressure Inflection Point Method

Pore size influences reservoir oil storage capacity, while throat size governs fluid flow capability within the reservoir. Displacement pressure, a key parameter in capillary pressure curves, refers to the pressure required to overcome the largest throat when the wetting phase fluid in a rock sample begins displacement by the non-wetting phase fluid. It reflects the minimum pressure needed for reservoir water displacement. Pore permeability is directly related to displacement pressure and can be used to determine the lower limit of reservoir properties. Based on mercury porosimetry data from 60 L-section cores in the study area, the relationship between displacement pressure and permeability was established (Figure 4). When permeability is less than 1.$^{8\times10^{-3}}\mu m^2$, the displacement pressure increases sharply. This indicates that formations with permeability below 1.$^{8\times10^{-3}}\mu m^2$ are unlikely to function as effective reservoirs. Therefore, the lower permeability limit for the L section is determined to be $1.^{8\times10^{-3}}\mu m^2$. Based on the porosity-permeability relationship derived from core analysis, the lower porosity limit for the L section is established as 9.14%.

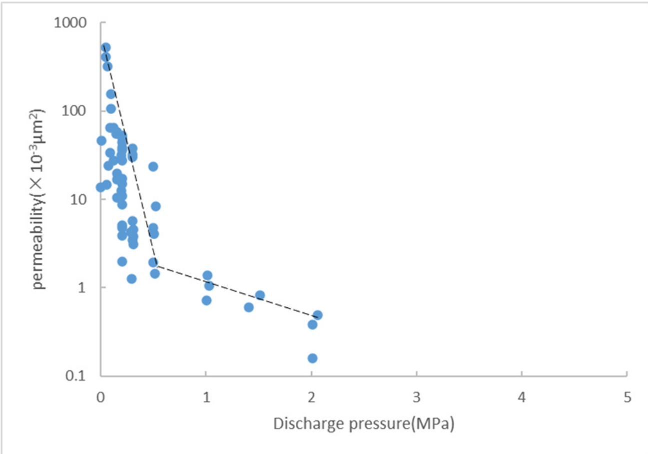

Figure 4. Displacement Pressure-Permeability Intersection Diagram

4.4. Minimum Flow Throat Radius Method

The macroscopic porosity and permeability characteristics of rock reflect its microscopic pore structure and throat size. Pores and throats in reservoir rocks provide the space and pathways for hydrocarbon accumulation and flow. The size of rock throat radii is a critical factor determining whether hydrocarbons can flow out of the rock under a certain pressure differential. The minimum throat radius that allows both hydrocarbon storage and flow is termed the minimum flowable throat radius [8,9].

Based on domestic and international research findings, a thickness of 0.1 μm roughly corresponds to the water film thickness adhering to the surface of water-wetted clastic rocks. During reservoir formation, oil and gas displacing water must overcome extremely high capillary pressures. When reservoir pore throats are smaller than 0.1 μm, oil and gas struggle to enter and form an effective reservoir. Therefore, 0.1 μm is considered the lower limit for reservoir pore throats. Based on mercury porosimetry experiments, statistical porosity, and permeability versus throat radius relationships (Figures 5, 6), the porosity corresponding to a 0.1μm throat radius is 8.12 ( ), which can serve as the lower porosity limit. The permeability corresponding to a 0.1μm throat radius is $2.^{02\times10^{-3}}\mu m^2$(), which can serve as the lower permeability limit.

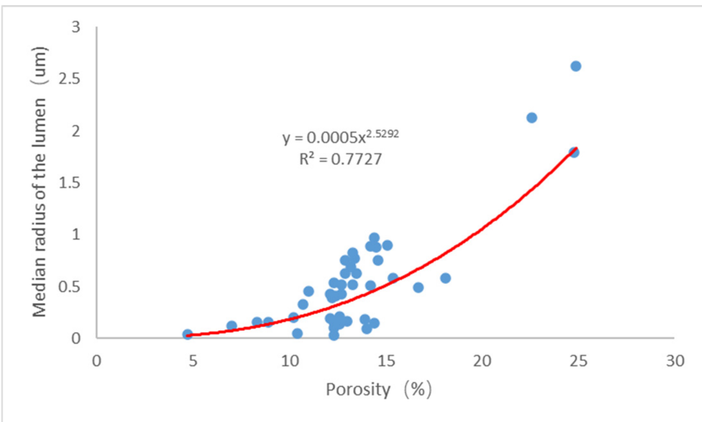

Figure 5. Pore Volume-Median Throat Radius Intersection Plot

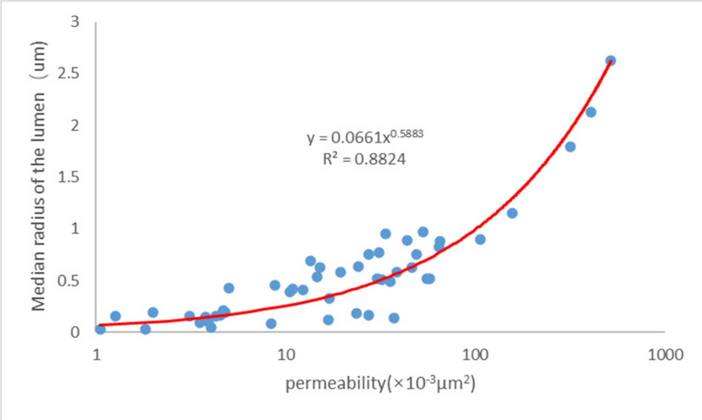

Figure 6. Porosity-Throat Median Radius Intersection Diagram

4.5. Verification of Lower Bound for Effective Reservoir Properties

This study employed multiple methods to determine the lower limits of reservoir properties for the L Formation in the Yaxia area. Although the principles of these methods differ, the resulting lower limit values show minimal variation, indicating that the lower limits established by all five methods are reasonable. The cumulative frequency method, minimum curvature radius method, and bound water saturation method collectively established the lower limits for the L-layer reservoir properties in the Yaxia area: a minimum porosity of 8.3% and a minimum permeability of $1.^{53\times10^{-3}}\mu m^2$.

Table 2. Lower Boundary Properties of L Formation in Yaxia Oilfield Determined by Integrated Methods

Method	Porosity (%)	Permeability ($\times10^{-3}\mu m^2$)
Cumulative Frequency Method	7.5	1.2
Minimum curvature radius method	9.57	1.53
Bound Water Saturation Method	7.0	1.1
Displacement Pressure Inflection Point Method	9.14	1.8
Minimum Flow Throat Radius Method	8.12	2.02
Average	8.305	1.53

5. Conclusion

When determining the lower limits of reservoir properties, due to limitations in geological data, different methods yield varying results. Each method has inherent limitations and specific applicability, with accuracy constrained by the richness of available data and information. Therefore, only by integrating various methods can the lower limits of reservoir properties be comprehensively studied. This study employs cumulative frequency analysis, minimum flow throat radius method, and confined water saturation method to determine lower limits. For the L Formation of the Baiyanghe Group in the Yaxia area, the lower limits are established as: minimum porosity of 8.2% and minimum permeability of $1.5^{\times10^{-3}\mu m^2}$.

Effective reservoirs in the L Formation of the Yaxia area are primarily controlled by sedimentary, diagenetic, and tectonic processes. Subaqueous distributary channels at the delta front and deltaic bars represent the most favorable microfacies types. Mechanical compaction and cementation both degrade reservoir properties, whereas soluble minerals like feldspar and carbonates erode in acidic environments to form secondary porosity, effectively enhancing reservoir properties. Additionally, tectonic processes exert a positive influence on reservoir properties. However, this study lacks quantitative characterization of how various dominant factors affect effective reservoirs.

ISSN: 2688-8645

References

[1] WU Weitao, ZHAO Jingzhou, WEI Xinshan, et al. Evaluation of gas-rich "sweet-spot" and controlling factors of gas-water distribution in tight sandstone gas provinces: an example from the Permian He 8 Member in Sulige Gas Province, central Ordos Basin, northern China [J]. Journal of Asian Earth Sciences, 2022, 227:105098.

[2] Zhang Yuxiang, Yang Shenglai, Wang Beidong, et al. Determining Lower Boundaries of Reservoir Properties in Ultra-Deep Carbonate Reservoirs Using Radial Flow Production Capacity Modeling: A Case Study of the Gaoshitai-Moxi Block [J]. Daqing Petroleum Geology and Development, 2023, 42(3): 75-82.

[3] Cheng Qi, Liu Zongbin, Wang Jianli, et al. Metamorphic Rock Subsurface Reservoir Structure and Its Production Dynamic Response: A Case Study of the Jinzhou 25-1 South Oilfield in the Bohai Sea [J]. Journal of Northeast Petroleum University, 2022, 46(1): 26-35.

[4] Li Wenhao, Zhang Zhihuan, Jiu Ling, et al. Lower Bound of Reservoir Properties and Controlling Factors for Effective Reservoirs in Gravels of the Shahejie Formation in the Northern Steep Slope Zone of the South Bohai Basin [J]. Petroleum and Natural Gas Geology, 2012, 33(5): 766-777.

[5] Cao Yingchang, Zhang Huina, Antuoklai, et al. Lower Bound of Effective Reservoir Properties and Controlling Factors in the Middle-Deep Layers of the Paleogene in the Southern Raoyang Depression [J]. Journal of Jilin University (Earth Science Edition), 2015, 45(6): 1567-1579.

[6] Zhu Yalin, Dong Hao, Liu Jinlong, et al. Study on the Lower Limit of Effective Thickness of the Chang 6 Reservoir in the Shangzhenzi Area [J]. Petroleum Geology and Engineering, 2016, 30(6): 69-72.

[7] Liu Zhidi, Shi Yujiang, Zhou Jinyu, et al. Review and Applicability Analysis of Methods for Determining Lower Limits of Effective Reservoir Properties [J]. Advances in Geophysics, 2018, 33(03): 1102-1109.

[8] Xu Huaixian, Li Jianzhong. Tight Oil: A New Hotspot in Global Unconventional Petroleum Exploration and Development [J]. Petroleum Exploration and Development, 2012, 39(1): 99-106.

[9] Jiang Yuqiang, Gao Yang, Xu Houwei, et al. Method for Determining Lower Bound of Physical Properties in Hydrophilic Low-Permeability Reservoirs Based on Starting Pressure Gradient: A Case Study of the Xujiahe Formation Gas Reservoir in the Baochang Area, Southern Sichuan [J]. Oil and Gas Geology and Recovery Rate, 2010, 17(5): 58-60.

[10] Cong Lin, Liu Yang, Ma Shizhong, et al. Application of Dynamic and Static Data in Determining Lower Limits of Effective Reservoir Properties in Tight Sandstones [J]. Contemporary Chemical Industry, 2014, 43(8): 1599-601, 1619.

[11] Lei Qihong, Sun Hualing, Li Jing, et al. Evaluation of Fluid Saturation in Low-Permeability Reservoirs at Changqing Oilfield [J]. Low-Permeability Oil and Gas Fields, 2006, 11(12): 94-97.

[12] An Zuoxiang. New Perspectives on the Formation of Laojunmiao Oilfield [J]. Xinjiang Petroleum Geology, 1998, 19(4): 265-269.